Omni-Directional Regeneration (ODR) of Gap Sensor Signal for Journal Bearing System Diagnosis

Joon Ha Jung[1], Byung Chul Jeon[2], Byeng D. Youn[3], Donghwan Kim[4], and Yeonwhan Kim[5]

[1,2,3]*Department of Mechanical and Aerospace Engineering, Seoul National University, Seoul, 151-919, Republic of Korea*

reallibero@gmail.com
puurni@empas.com
bdyoun@snu.ac.kr

[4,5]*Power Generation Laboratory, KEPCO Research Institute, 305-760, Republic of Korea*

kimdonghwan@kepco.co.kr
90101552@kepco.co.kr

ABSTRACT

We have developed a technique that enhances the detectability of sensors used to acquire data from a journal bearing rotor system. Usually, at an axial position for the rotating shaft on a journal bearing system, two sensors are fixed in radial direction at a right angle. The conventional diagnosis researches use only the acquired signals. However, two fixed sensors may not give sufficient information for diagnosis of the system since anomalies can happen in arbitrary direction. To improve the robustness of the diagnosis, coordinate transformed gap sensor signal is generated in arbitrary direction without installing extra sensors or adjusting sensor positions. With the original signals, the generated signals are used in the process of diagnosis. The powerful but simple method is described in the paper, and is verified by data sets from the experiment.

1. INTRODUCTION

The journal bearing supports rotating parts of the mechanical systems with a fluid. Since the fluid ensures smooth rolling of the rotors, it is frequently used in large systems that require safe operation. For example, turbines and pumps in power plants use journal bearings to maintain the systems safely in heavy load and high speed conditions. Without a direct contact between the rotor and the stator, the vibration can be kept below in a certain magnitude. Apart from the stability of the journal bearings, a large rotor system requires an anomaly diagnosis system. Although the design of the rotor systems satisfy the requirements of the system, uncertainties can arouse from operation as well as manufacturing process. These uncertainties in the rotor systems cause the system to operate in an unexpected way. Sometimes, a sudden failure or an accident can happen if proper maintenance action is not performed and the consequence can be disastrous. Thus, to prevent such unfortunate events and to take proper measures based on the exact condition of the system, diagnosis systems are commonly installed in large rotor systems.

The diagnosis systems for rotors use data-driven method frequently. The method follows the steps: data acquisition, feature generation, and classification. First, the signals from each health state are obtained. Most of the signals for rotors use vibration signals since they can well represent the state of the operating condition. Then the obtained signals are processed by appropriate techniques. Next, the processed data are used to extract features that represent each health state and the condition of the rotors. With the extracted features, a classifier is trained, and the classifier classifies newly acquired data after following the same steps as the training data.

Among the stated steps, various signal processing techniques are developed to generate features of good separation ability, which eventually leads to accurate diagnosis results. Examples of various signal processing methods for vibration data are angular resampling (Bonnardot, El Badaoui, Randall, Daniere, & Guillet, 2005; Villa, Reñones, Perán, & De Miguel, 2011), statistical approach (Jeon, Jung, Youn, Kim, & Bae, 2014), principal component analysis (Malhi & Gao, 2004; Sun, Chen, & Li, 2007), and wavelet transform (Liu, 2003; Sanz, Perera, & Huerta, 2007). However, the gap sensors are mostly fixed in the rotor systems and the sensor location is hard to adjust. Due to the fixed location of the sensors, the diagnosis accuracy of direction oriented anomalies (e.g. rubbing, misalignment) may be demanding. Researches have been conducted to resolve the limitation of the fixed location of sensors. Orbit identification in time-

domain and full-spectrum in frequency-domain are the two methods.

The orbit information can be obtained since most of the rotor systems have two sensors in a right angle. Yan, Zhang, Li, Li, and Huang (2009) modified the orbit into seven different features to identify the state of the steam turbine generator. H. Wang, Wang, and Ji (2013) quantified the orbit information with isometric feature mapping to identify faults in rotors. Other researches also tried to quantify the orbit shape to make more accurate diagnosis of rotors (Bachschmid, Pennacchi, & Vania, 2004; Bo, Jian-Zhong, Wen-Qing, & Bing-Hui, 2004; C. Wang, Zhou, Kou, Luo, & Zhang, 2012; Yan, Zhang, & Wu, 2010). Full-spectrum analysis uses both x- and y- signals to expresses the forward and backward frequency of the rotors (Chen & Chen, 2011; Goldman & Muszynska, 1999; T. H. Patel & A. K. Darpe, 2009; Patel & Darpe, 2011; Zhao, Patel, & Zuo, 2012). Fengqi and Meng (2006), and T. Patel and A. Darpe (2009) tried to detect rubbing state by using full-spectrum.

However, full-spectrum as well as orbit identification are not enough to represent thorough information of each state. Quantification of the orbit information varies from papers to papers, and the quantification process has huge effects on the overall performance of diagnosis. Full-spectrum uses x- and y- signals acquired from the fixed gap sensors, but the two signals may not be enough to represent the direction-oriented anomalies. To overcome these limits and to make robust diagnosis system, we have suggested omni-directional regeneration (ODR) technique to enhance the robustness of the various anomalies.

The paper is organized as follows. Section 2 briefly states overview of journal bearing diagnosis system. Section 3 describes the experiment set-up used in this research. Section 4 states procedures of ODR based diagnosis. Section 5 shows the results of ODR based diagnosis. In section 6, short summary of the research and future works are stated.

2. OVERVIEW OF JOURNAL BEARING DIAGNOSIS SYSTEM

This section describes general procedures of journal bearing diagnosis. Section 2.1 describes the characteristics of gap sensor signals used. Section 2.2 describes diagnosis process based on supervised-learning.

2.1. Gap Sensor Signals in Journal Bearing Systems

The proximity sensors, also known as gap sensors, are widely used in journal bearing systems because the system operates in a low level of vibration, and thus require high resolution sensors. The high resolution of the gap sensor is possible as it measures the change of the eddy current. The vibration signals are acquired as voltage. Alternating current (AC) component of the voltage represents relative vibration, while direct current (DC) component represents absolute radial position of the rotor. Generally, two gap sensors are placed in the same axial location at a right angle to show orbit of the rotor as presented in Figure 1.

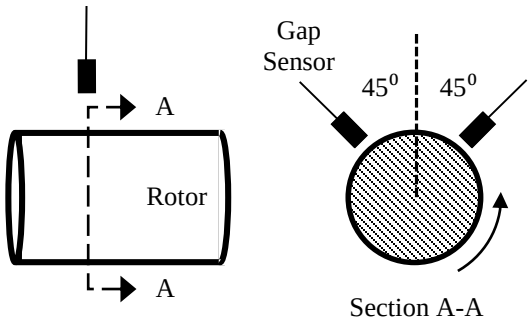

Figure 1. Gap Sensors in Rotor.

2.2. Diagnosis Process Based on Supervised-Learning

The supervised learning method is commonly used in diagnosis process of journal bearing systems. The acquired vibration signals from the gap sensors are used to generate features. The feature generation includes feature selection as well as extraction. Then an appropriate classifier is trained and is used to classify the system into health states. The following subsections describe the feature generation and the classification.

2.2.1. Feature Generation

Feature generation, which can be divided into feature extraction and selection processes, has significant effect on the performance of diagnosis. Since the research targets on steady-state system, time- and frequency- domain features rather than time-frequency domain features are used. The candidate features listed in Table 1 and 2 are widely used ones in detecting the faults or abnormality of rotor systems (Jeon et al., 2014; Sun et al., 2007). Time-domain features include statistical moments and waveform related features. Frequency-domain features include various frequency spectrum features which are closely related to the state of the rotor system.

Total of sixteen features were extracted from the vibration signals. Before extracting the features, angular resampling was applied to the raw vibration signals to enhance the separation ability of the features and to reduce the noise. From the resampled signals, time-domain features were extracted by one cycle basis, while freq.-domain feature by sixty cycle basis (Jeon et al., 2014).

Among the extracted features, optimal features are selected by using the genetic algorithm. Features have different ability in health state separation, so not every feature listed in Table 1 and 2 guarantee accurate diagnosis result. For example, a specific feature can represent the oil whirl very well, but it may not tell difference between normal and rubbing states. In

addition, highly correlated features are redundant features that can be reduced. The optimal feature subset of k number of features was obtained by finding a subset that maximizes the following fitness function, f_n, presented as:

$$f_n = (1-\alpha) \times mean(MI) - \alpha \times \frac{1}{{}_kC_2} \sum_{i,j=1,i\neq j}^{k} \left|\rho_{i,j}\right| \quad (1)$$

Table 1. Time-domain Features.

Number	Contents	Description
1	Skewness	$\frac{\sum(X_i - \bar{X})^3}{(N-1)s^3}$
2	Kurtosis	$\frac{\sum(X_i - \bar{X})^4}{(N-1)s^4}$
3	Crest Factor	$\mathrm{Max}(\lvert X_i \rvert) \times \sqrt{\frac{N}{\sum {X_i}^2}}$
4	Shape Factor	$\sqrt{\frac{\sum {X_i}^2}{N}} \times \frac{N}{\sum \lvert X_i \rvert}$
5	Impulse Factor	$\mathrm{Max}(\lvert X_i \rvert) \times \frac{N}{\sum \lvert X_i \rvert}$

Table 2. Frequency-domain Features.

Number	Contents	Description
6	FC	$\frac{\int f \times s(f) df}{\int s(f) df}$
7	RMSF	$\left[\frac{\int f^2 \times s(f) df}{\int s(f) df}\right]^{1/2}$
8	RVF	$\left[\frac{\int (f-FC)^2 \times s(f) df}{\int s(f) df}\right]^{1/2}$
9	0.5X / 1X	$\sqrt{s(f_{0.5X})/s(f_{1X})}$
10	2X / 1X	$\sqrt{s(f_{2X})/s(f_{1X})}$
11	(1x~10x)/1x	$\left\{\sum_{n=1}^{10} \sqrt{s(f_{nX})}\right\} / \sqrt{s(f_{1X})}$
12	(0~0.39x)/1x	$\left\{\int_0^{0.39X} \sqrt{s(f)}\, df\right\} / \sqrt{s(f_{1X})}$
13	(0.4x~0.49x)/1x	$\left\{\int_{0.4X}^{0.49X} \sqrt{s(f)}\, df\right\} / \sqrt{s(f_{1X})}$
14	(0.51x~0.99x)/1x	$\left\{\int_{0.5X}^{0.99X} \sqrt{s(f)}\, df\right\} / \sqrt{s(f_{1X})}$
15	(3x~5x)/1x	$\left\{\int_{3X}^{5X} \sqrt{s(f)}\, df\right\} / \sqrt{s(f_{1X})}$
16	(3x,5x,7x,9x)/1x	$\left\{\sum_{n=1}^{4} \sqrt{s(f_{2n+1X})}\right\} / \sqrt{s(f_{1X})}$

where $mean(MI)$ is the average of mutual information between the feature and the class, $\rho_{i,j}$ is the correlation coefficient between i^{th} and j^{th} features, α is the penalty coefficient, k is the user defined number of features for the optimal subset, and n indicates the n^{th} feature subset among N number of subsets in a generation (Guo, Damper, Gunn, & Nelson, 2008). The mutual information represents the separation ability of the features, and the correlation coefficient represents redundant features.

2.2.2. SVM Classification

The supervised learning method frequently uses support vector machine (SVM) algorithm for the classification step because of its simple and strong performance. First, the classifier is trained by using the optimal features acquired via feature generation process. Only the feature data with known class is used for training the classifier. The trained classifier denotes a hyper-plane that maximizes the margin between the classes. After the classifier is trained, the feature data with unknown class is tested. The testing predicts the class of feature data. In this research, the known feature data is used for the testing step, and the predicted class was compared to the actual class to evaluate the performance of the classifier.

Although SVM was originally designed for linearly separable two-class problem, it can be used for non-linear two-class problem by introducing the slack variable and the kernel function. Furthermore, by applying one-against-one (OAO) decision method, SVM can be expanded to classify multi-class problem. In this research, the LIBSVM algorithm was used (Chang & Lin, 2011).

3. DIAGNOSIS METHODOLOGY USING OMNI-DIRECTIONAL REGENERATION

This section describes the ODR signal based diagnosis procedures. Most of the diagnosis procedures follow as in section 2, but few steps are modified and adjusted as described in this section. Section 3.1 defines ODR signals, and section 3.2 describes how ODR signals are used in the diagnosis procedure.

3.1. Omni-Directional Regeneration of Gap Signals

3.1.1. Definition of ODR

The principal of ODR signal generation is the transform of the coordinate system as presented in Figure 2. The clock-wise transform of a data point (x_1, y_1) in two-dimension Cartesian coordinate system can be expressed as:

$$\begin{bmatrix} x_2 \\ y_2 \end{bmatrix} = \begin{bmatrix} cos\theta & -sin\theta \\ sin\theta & cos\theta \end{bmatrix} \times \begin{bmatrix} x_1 \\ y_1 \end{bmatrix} \quad (2)$$

where θ denotes degree of rotation, and x_2 & y_2 denotes the data point in θ rotated coordinates system.

The scalar data values, x_i and y_i, in equation (2) can be replaced by vectors, $\boldsymbol{x}_i$ and $\boldsymbol{y}_i$, as:

$$\boldsymbol{x_2} = cos\theta \boldsymbol{x_1} - sin\theta \boldsymbol{y_1} \quad (3)$$

$$\boldsymbol{y_2} = sin\theta \boldsymbol{x_1} + cos\theta \boldsymbol{y_1} \quad (4)$$

where $\boldsymbol{x}_i$ and $\boldsymbol{y}_i$ are vectors in i^{th} coordinate system. The vibration signals from the sensors (a) and (b) in Figure 3 can be indicated by $\boldsymbol{x}_1$ and $\boldsymbol{y}_1$, respectively. Then, the coordinate transformed signals by θ, $\boldsymbol{x}_2$ and $\boldsymbol{y}_2$, can be regarded as the signals obtained from sensors (c) and (d), respectively.

Using this principle, the ODR signals, $\boldsymbol{x}_n$ and $\boldsymbol{y}_n$, can be defined as:

$$\begin{aligned} \boldsymbol{x_n} &= \cos(n\Delta\theta)\, \boldsymbol{x}_0 - sin(n\Delta\theta)\boldsymbol{y}_0 \\ \boldsymbol{y_n} &= \sin(n\Delta\theta)\, \boldsymbol{x}_0 + cos(n\Delta\theta)\boldsymbol{y}_0 \\ & (n = 1, 2, \dots, N) \end{aligned} \quad (5)$$

where $\boldsymbol{x}_0$ and $\boldsymbol{y}_0$ are the acquired vibration signals from gap sensors, $\Delta\theta$ is the increment of the rotation angle, and N ($=\lfloor \pi/\Delta\theta \rfloor$) is the maximum number of ODR that can be generated.

The ODR can generate vibration signals from an arbitrary direction. Multiple ODR signals around the rotor can be obtained by adjusting the increment of the angle, $\Delta\theta$. To diagnose the state of the system accurately, $\Delta\theta$ should be fine. However, if $\Delta\theta$ is too fine, the number of ODR signals (N) will increase, and the computational load will also increase. Thus the increment of the angle, $\Delta\theta$, is set as $\pi/16$ in this research. In addition, the vibration signals are radial symmetric, so ODR signals within the π rotation angle range will be generated. Likewise, there is no need to use both $\boldsymbol{x}_n$ and $\boldsymbol{y}_n$, because $\boldsymbol{x}_n$ signal is equal to $\boldsymbol{y}_{n+8}$, which is 90° rotated signal of $\boldsymbol{y}_n$. The $\boldsymbol{x}_n$ covers all $\boldsymbol{y}_n$ if ODR covers more than half rotation.

3.1.2. Validation of ODR

To check that ODR signals truly represent the signal acquired from rotated direction, three evidences are provided by the example vibration signals.

First, $\boldsymbol{x}_8$ which is 90° counter-clockwise (ccw) ODR signal of $\boldsymbol{x}_0$ exactly matched to $\boldsymbol{y}_0$. As shown in Figure 4, the two signals are identical to each other. Second, $\boldsymbol{x}_0$ is located in the opposite direction of $\boldsymbol{y}_8$, so the signals were in reverse of each other. This is also shown in Figure 4. Last, the orbit shape remained the same for any $\boldsymbol{x}_n$ and $\boldsymbol{y}_n$. This is shown in Figure 5 that the orbit shape is consistent over rotation angle. Thus from the three evidences, the ODR signals exactly shows behavior of the rotor in arbitrary angle.

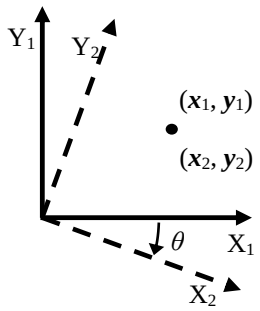

Figure 2. Coordinate transformation of a point in two-dimensional system.

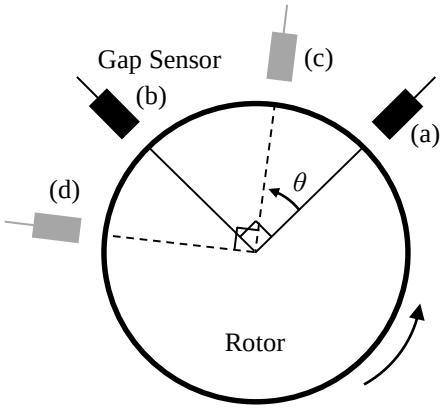

Figure 3. Gap sensor and virtual sensors.

3.2. Diagnosis Procedures using ODR Signals

3.2.1. Feature Extraction and Reduction

Each ODR signal generates sixteen features defined in section 2.2.1, which makes 16 × N features in total. Since the number of ODR, N, was set as sixteen, total number of features add up to 256. But not all 256 features are useful in classification of health states, so the number of features are reduced by Principal Component Analysis (PCA) (Malhi & Gao, 2004).

PCA decorrelates the multi-dimension features by finding coordinates of principal components. The principal components, v_i, are derived by solving the following equation:

$$\begin{aligned} Av_i &= \lambda_i v_i \\ & (i = 1,2, \dots,256) \end{aligned} \quad (6)$$

where A is the covariance matrix of feature vectors and λ_i is indices, $\underline{i}$, are sorted in descending order of eigenvalues. The projection matrix, $\boldsymbol{V}$, is defined as equation (7) (Sun et al., 2007).

$$\boldsymbol{V} = [v_1, v_2, \dots, v_{256}] \quad (7)$$

By multiplying $\boldsymbol{V}$ to the feature vectors, new de-correlated features are obtained.

However, not all the de-correlated features have good separation ability. Among the 256 new features, ones that had variances larger than one were used, which counts for ten features. Thus principal components corresponding to ten largest eigenvalues are used in this research. Consequently, 256 ODR features were reduced to ten features by PCA.

3.2.2. Feature Selection and Classification

The ten reduced features by PCA are used for feature selection process. As stated in Section 2.2.1, the number of features for optimal subset, *k*, should be defined prior to feature selection. Since the number of reduced features are ten, *k* ranges from two to ten. For each *k*, feature selection was performed. Then, the selected features were used for classification process as stated in Section 2.2.2. To validate the effectiveness of ODR, the classification results of non-ODR signals were also performed. The results are presented in Section 5.

4. DESCRIPTION ON EXPERIMENT

4.1. Test-bed Description

The research is based on the data acquired from the experiment. The experiment was conducted on the RK4 test-bed made by GE Bently-Nevada. Four health states—normal, rubbing, misalignment, oil whirl—were tested on RK4. First, the normal health state was tested with two shafts. A short and a long shaft of 10mm diameter were connected by a flexible coupling, and the short shaft was driven by the motor. An 800 gram disc was attached at the middle of the long shaft supported by two bearings. The amplitude of vibration was set to a certain level by balancing procedure. Second, the rubbing state also had the same set-up as that of normal, but the rubbing screw induced direct point contact on the shaft at steady-state. An accelerometer was attached to the screw jig to maintain the consistent level of the rubbing. For the misalignment state, a special jig was added to the normal set-up to shift the shorter shaft horizontally, which represents an angular misalignment. An exact amount of misalignment was controlled by the jig. For the last health state, oil whirl, one shaft and two discs were used to enforce whirling force at the end of the shaft. The pressure of oil in the bearing was controlled to produce whirling in the bearing.

4.2. Data Acquisition

All four health states were tested for sixty-seconds to obtain enough amount of data. Since the speed of the rotor was 3,600 rpm, sixty-seconds of test can collect 3,600 cycles of vibration. In addition, each health state was repeated twice, which adds up to three sets, to apply cross-validation.

The displacement of the shaft was obtained by Bently Nevada 3300 proximity sensors. The two sensors in a right angle were

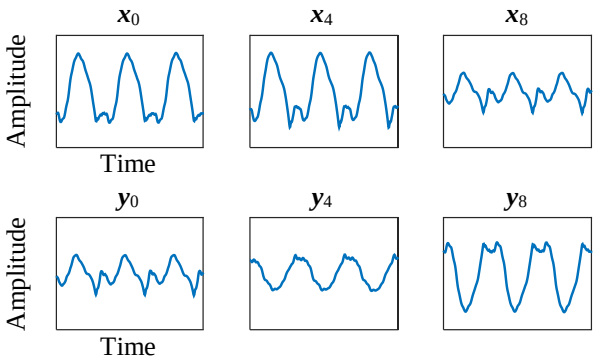

Figure 4. Example of ODR signals.

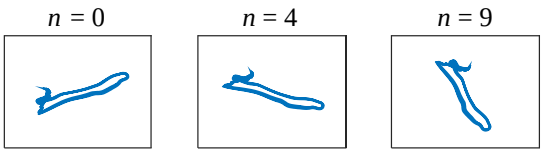

Figure 5. Example of ODR signal orbits.

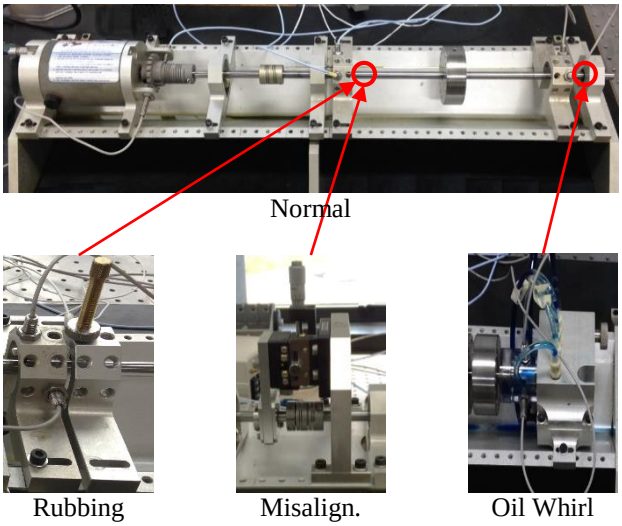

Figure 6. Set-up of RK4 test-bed.

placed at an axial location adjacent to the anomaly position. Additionally, tacho signal was measured to acquire the phase of the rotating shaft, and was used in the resampling process. All three signals were acquired through NI DAQ 4432.

5. RESULTS AND DISCUSSION

5.1. Qualitative Analysis

The four health states were tested on RK4 test-bed. Graphical representations such as orbits are widely used to distinguish each health state. Two cycles of orbits are represented in

Figure 7. Rotors in a normal state rotates smoothly, so the orbit of normal is close to a clear circle. The orbit of rubbing state shows trace of contact between the rubbing screw and the shaft. Misalignment has preloaded shaft, and this is characterized by two small circles. Oil whirl health state shows orbits of incomplete circles, a typical sign of sub-harmonic dominant signals.

As shown in Figure 8, the rubbing and misalignment show characteristics of direction oriented health states. The ODR signals of direction oriented anomalies change over the rotation angle. However, the conventional method only uses the acquired signals, $\boldsymbol{x}_0$ and $\boldsymbol{y}_0$. Therefore, the performance of the classification may depend on the anomaly directions.

5.2. Quantitative Analysis

The effectiveness of the ODR signals with PCA feature reduction can be evaluated by class prediction results. The results are compared for all the number of possible optimal feature subset, *k*. As described in section 3.2.2, the *k* ranged from two to ten. In addition, as stated in section 4.2, *leave-one-out cross-validation* was performed. Since three datasets were acquired through experiment, two sets were used to train classifier and the other one set was used as testing data. The three graphs in Figure 9 correspond to each case of cross-validation.

The two dotted lines in Figure 9 are the results using $\boldsymbol{x}_0$ and $\boldsymbol{y}_0$ signals, while the single line is the results using ODR signals with PCA. The dotted lines represent the conventional data-driven method using only the signals acquired from the sensors. On the other hand, the single lines represent the results using ODR signals. The ODR signal not only uses the acquired signals but also signals in other directions. Thus the sixteen ODR signals can characterize health state of the system more accurately, and eventually gives enhanced results.

The (a), (b), and (c) in Figure 9 represent each case of the classification results of cross-validation. When number of optimal features were larger than three, the ODR signal based method predicted the testing data 100% accurate. In contrast to that, the results by the $\boldsymbol{x}_0$ and $\boldsymbol{y}_0$ signals are not consistent. The (a) case shows that the prediction accuracy increases as the number of features are increased, and 100% accuracy is obtained when five or more features are used. However, in (b), the accuracy of $\boldsymbol{x}_0$ signals oscillates. Moreover, the accuracy of $\boldsymbol{y}_0$ signals are relatively lower in (b) and (c). This results indicate that conventional method of using the acquired signals cannot guarantee good results, whereas ODR signals can give good results consistently regardless of direction of anomalies and sensors.

6. CONCLUSION

This research was conducted to enhance the diagnose performance on the health state of journal bearing systems. The data used in this study were acquired from RK4 test-bed. For non-direction oriented health states, normal and oil whirl were selected, whereas rubbing and misalignment were selected for direction oriented health states. From the two acquired signals, ODR signals were generated for each health state. The generated ODR signals represented vibration signals around the rotor, and all the signals were turned into time- and frequency- domain features. The sixteen features of sixteen ODR signals piled to 256 features, then the features were reduced by PCA. Finally feature selection and classification were performed. To add reliability to the study, *leave-one-out cross-validation* was performed on the three data sets.

We have suggested PCA based ODR method to diagnose the journal bearing rotor system. To the best of our knowledge, no research had tried to generate vibration signals based on the two signals in a right angle. This method is useful for characterizing the direction oriented health states as well as non-direction oriented ones. Characterizing the health states successfully lead to accurate diagnosis results, while signals without ODR presented inconsistent diagnosis results.

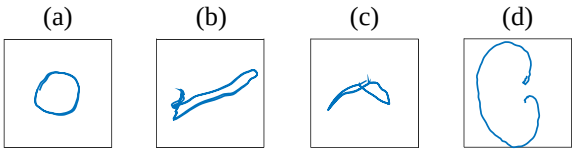

Figure 7. Two cycle orbits of (a) normal, (b) rubbing, (c) misalignment, and (d) oil whirl.

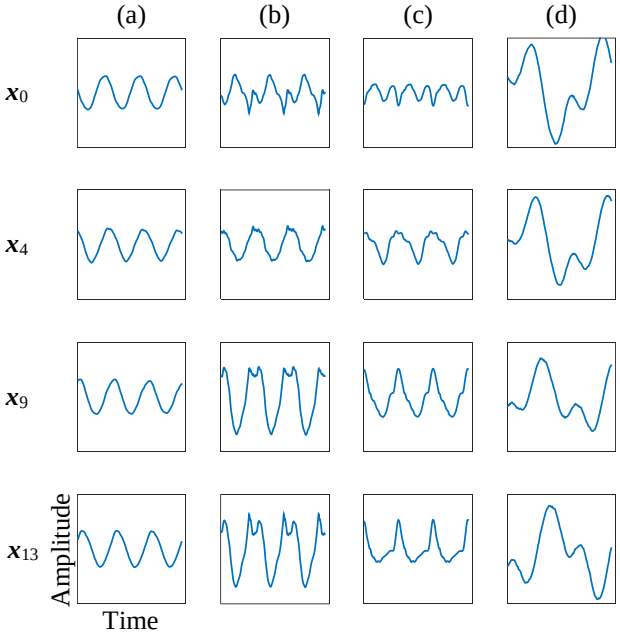

Figure 8. ODR signals of (a) normal, (b) rubbing, (c) misalignment, and (d) oil whirl.

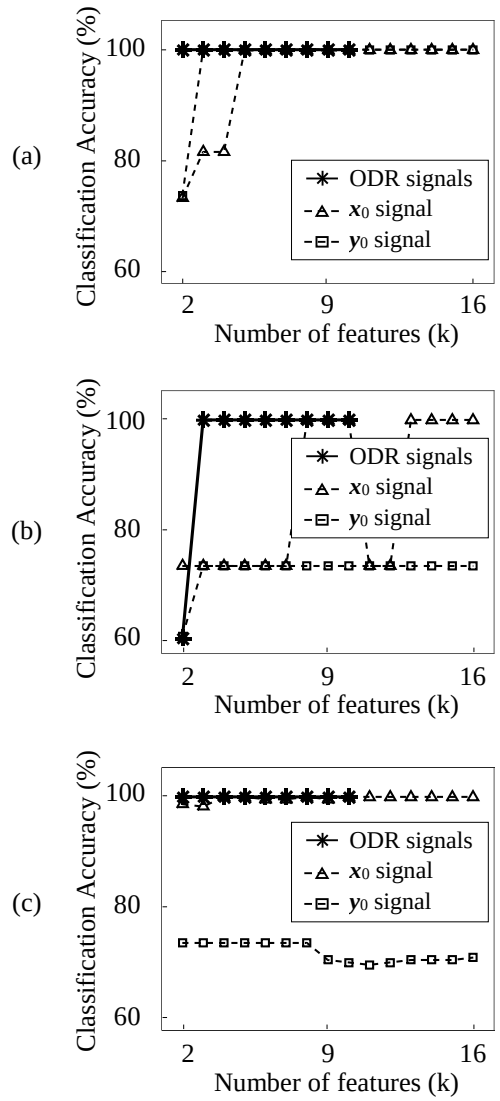

Figure 9. Classification results by x_0, y_0, and ODR signals

For future works, study regarding the optimal number of ODR signals should be defined considering the computational resources and the accuracy of diagnosis. In other words, optimal $\Delta\theta$ is to be determined using appropriate method. Furthermore, correlation among the ODR signals can be considered to reduce computational loads of calculating ODR signals.

ACKNOWLEDGEMENT

This work was supported by Mid-career Researcher Program through the National Research Foundation of Korea (NRF) grant funded by the Ministry of Science ICT and Future Planning (MSIP) (2013R1A2A2A01068627). This work was also supported by the Power Generation & Electricity Delivery Core Technology Program of the Korea Institute of Energy Technology Evaluation and Planning (KETEP) granted financial resource from the Ministry of Trade, Industry & Energy, Republic of Korea (No. 2012101010001C).

REFERENCES

Bachschmid, N., Pennacchi, P., & Vania, A. (2004). Diagnostic significance of orbit shape analysis and its application to improve machine fault detection. *Journal of the Brazilian Society of Mechanical Sciences and Engineering*, vol. *26*, pp. 200-208.

Bo, F., Jian-Zhong, Z., Wen-Qing, C., & Bing-Hui, Y. (2004). Identification of the shaft orbits for turbine rotor by modified Fourier descriptors. *Machine Learning and Cybernetics, 2004. Proceedings of 2004 International Conference on*, 26-29 Aug. 2004.

Bonnardot, F., El Badaoui, M., Randall, R., Daniere, J., & Guillet, F. (2005). Use of the acceleration signal of a gearbox in order to perform angular resampling (with limited speed fluctuation). *Mechanical Systems and Signal Processing*, vol. *19*(4), pp. 766-785.

Chang, C.-C., & Lin, C.-J. (2011). LIBSVM: A library for support vector machines. *ACM Trans. Intell. Syst. Technol.*, vol. *2*(3), pp. 1-27.

Chen, C.-S., & Chen, J.-S. (2011). Rotor fault diagnosis system based on sGA-based individual neural networks. *Expert Systems with Applications*, vol. *38*(9), pp. 10822-10830.

Fengqi, W., & Meng, G. (2006). Compound rub malfunctions feature extraction based on full-spectrum cascade analysis and SVM. *Mechanical Systems and Signal Processing*, vol. *20*(8), pp. 2007-2021. doi: 10.1016/j.ymssp.2005.10.004

Goldman, P., & Muszynska, A. (1999). Application of full spectrum to rotating machinery diagnostics. *Orbit*, vol. *20*(1), pp. 17-21.

Guo, B., Damper, R. I., Gunn, S. R., & Nelson, J. D. B. (2008). A fast separability-based feature-selection method for high-dimensional remotely sensed image classification. *Pattern Recognition*, vol. *41*(5), pp. 1653-1662.

Jeon, B., Jung, J., Youn, B. D., Kim, Y., & Bae, Y. C. (2014). Statistical Approach to Diagnostic Rules for Various Malfunctions of Journal Bearing System Using Fisher Discriminant Analysis. *Second European Conference of the PHM Society 2014*, July 8-10, Nantes, France.

Liu, B. (2003). Adaptive harmonic wavelet transform with applications in vibration analysis. *Journal of Sound and Vibration*, vol. *262*(1), pp. 45-64. doi: http://dx.doi.org/10.1016/S0022-460X(02)01027-1

Malhi, A., & Gao, R. X. (2004). PCA-based feature selection scheme for machine defect classification. *IEEE*

Transactions on Instrumentation and Measurement, vol. *53*(6), pp. 1517-1525. doi: 10.1109/TIM.2004.834070

Patel, T., & Darpe, A. (2009). Use of full spectrum cascade for rotor rub identification. *Adv. Vib. Eng*, vol. *8*, pp. 139-151.

Patel, T. H., & Darpe, A. K. (2009). Experimental investigations on vibration response of misaligned rotors. *Mechanical Systems and Signal Processing*, vol. *23*(7), pp. 2236-2252.

Patel, T. H., & Darpe, A. K. (2011). Application of full spectrum analysis for rotor fault diagnosis. *IUTAM Symposium on Emerging Trends in Rotor Dynamics*.

Sanz, J., Perera, R., & Huerta, C. (2007). Fault diagnosis of rotating machinery based on auto-associative neural networks and wavelet transforms. *Journal of Sound and Vibration*, vol. *302*(4–5), pp. 981-999. doi: http://dx.doi.org/10.1016/j.jsv.2007.01.006

Sun, W., Chen, J., & Li, J. (2007). Decision tree and PCA-based fault diagnosis of rotating machinery. *Mechanical Systems and Signal Processing*, vol. *21*(3), pp. 1300-1317. doi: doi.org/10.1016/j.ymssp.2006.06.010

Villa, L. F., Reñones, A., Perán, J. R., & De Miguel, L. J. (2011). Angular resampling for vibration analysis in wind turbines under non-linear speed fluctuation. *Mechanical Systems and Signal Processing*, vol. *25*(6), pp. 2157-2168.

Wang, C., Zhou, J., Kou, P., Luo, Z., & Zhang, Y. (2012). Identification of shaft orbit for hydraulic generator unit using chain code and probability neural network. *Applied Soft Computing*, vol. *12*(1), pp. 423-429. doi: 10.1016/j.asoc.2011.08.028

Wang, H., Wang, H., & Ji, Y. (2013). Orbit identification method based on ISOMAP for rotor system fault diagnosis. *2013 IEEE 11th International Conference on Electronic Measurement & Instruments (ICEMI)*, 16-19 Aug. 2013.

Yan, C., Zhang, H., Li, H., Li, Y., & Huang, W. (2009). Automatic Identification of Shaft Orbits for Steam Turbine Generator Sets. *WRI Global Congress on Intelligent Systems, 2009. GCIS '09.* , 19-21 May 2009.

Yan, C., Zhang, H., & Wu, L. (2010). Automatic Recognition of Orbit Shape for Fault Diagnosis in Steam Turbine Generator Sets. *Journal of Computational Information Systems*, vol. *6*(6), pp. 1995-2008.

Zhao, X., Patel, T. H., & Zuo, M. J. (2012). Multivariate EMD and full spectrum based condition monitoring for rotating machinery. *Mechanical Systems and Signal Processing*, vol. *27*(0), pp. 712-728. doi: http://dx.doi.org/10.1016/j.ymssp.2011.08.001

BIOGRAPHIES

Joon Ha Jung received B.S. degree of mechanical engineering from Seoul National University (SNU) in 2012, and is involved in graduate School of Mechanical and Aerospace Engineering at SNU. He is currently doing research on Prognostics and Health Management for rotating machinery.

Byung Chul Jeon received the B.S. degree of aerospace engineering from Republic of Korea Air Force Academy in 2001 and the M.S. degree of mechanical engineering from Seoul National University in 2009. He is now a Ph. D. student at the School of Mechanical and Aerospace Engineering in Seoul National University. His current research is focused on the data driven Prognostics and Health Management for rotating machinery.

Byeng D. Youn received his Ph.D. degree from the department of Mechanical Engineering at the University of Iowa, Iowa City, IA, in 2001. He was a research associate at the University of Iowa (until 2004), an assistant professor in Michigan Technical University (until 2007), and an assistant professor in the University of Maryland College Park (until 2010). Currently, he is an associate professor at the School of Mechanical and Aerospace Engineering at Seoul National University, Republic of Korea. His research is dedicated to well-balanced experimental and simulation studies of system analysis and design, and he is currently exploring three research avenues: system risk-based design, prognostics and health management (PHM), and energy harvester design. Dr. Youn's research and educational dedication has led to: six notable awards, including the ISSMO/Springer Prize for the Best Young Scientist in 2005 from the International Society of Structural and Multidisciplinary Optimization (ISSMO), and more than 100 publications in the area of system-risk-based design, PHM and energy harvester design

Donghwan Kim received B.S degree from the department of mechanical engineering at the University of Inha, Incheon and the M.S degree from the department of mechanical engineering from Korea Advanced Institute of Science and Technology, Daejeon, in 2012. Currently, he is an associate researcher at Korea Electric power Research Institute, Daejeon, Korea. His research interests are fault detection, fault diagnosis, and failure prognosis of power plant systems and their applications.

Yeon-Whan Kim received his BS and MS degree from the department of Mechanical Engineering from Ajou University in 1987 and 1990, and his Ph.D. degree from the department of Mechanical Design Engineering at Chungnam National University in 2008, Korea. He is a Principal Researcher at Power Generation Laboratory in KEPCO Research Institute. His research is dedicated to machinery vibration analysis, noise analysis, mechanism identification on flow induced vibration, health condition monitoring and diagnostics in power plants. His current research is focused on prognostics and health management of rotating machinery in 1000MW class thermal power plant.